

H α as a Chromospheric Diagnostic

Robert J. Rutten^{1,2}

¹*Sterrekundig Instituut, Utrecht University, The Netherlands*

²*Institutt for Teoretisk Astrofysikk, University of Oslo, Norway*

Abstract. I first illustrate with images from the Dutch Open Telescope (DOT) that H α is the principal diagnostic of the solar chromosphere. The DOT movies at <http://dot.astro.uu.nl> demonstrate this fact even more vividly.

I then summarize, on the basis of the recent numerical simulations by Leenaarts et al. (2007), why H α is such an omnipresent diagnostic of the chromosphere. The ubiquity of H α fibrils in both hot and cool gas is due to (i) – the presence of shocks everywhere, guided by the magnetic field into dynamic fibrils near the network and pushing the canopy and transition region upward in weaker-field internetwork regions, (ii) – the large rate difference between the fast hydrogen ionization/recombination balancing in hot shocks and the slow balancing in cool post-shock gas, and (iii) – the large excitation energy of H α 's $n=2$ lower level, causing strong coupling to the ion population. These three facts combine to cause appreciable H α opacity throughout the chromosphere, enormously in excess of instantaneous Saha-Boltzmann partitioning in cool post-shock gas. Thus, sluggish post-shock recombination causes H α to be visible everywhere.

Finally, I address H α observing. Since *Hinode*'s H α imaging is affected by bubbles and limited in cadence, the DOT may serve as a complementary facility furnishing profile-sampling H α image sequences at the same 0.3 arcsec angular resolution as *Hinode* whenever the La Palma seeing is good. However, imminent loss of DOT funding requires outside financing of an on-site observer for DOT utilization in co-pointed joint observing.

1. The H α Chromosphere

Figure 1 portrays the chromosphere. The lower image, taken in Ca II H, shows a mixture of photospheric contributions (reversed granulation and acoustic grains) and chromospheric contributions (bright plage, network, and hedge-row straws) sampled by the centre and inner wings of this line. Ca II H is presently *Hinode*'s best chromospheric diagnostic but it shows the chromosphere only partially. The upper image shows the same scene in H α line centre. It makes obvious that H α presents a much more complete proxy to delineate chromospheric topology. The ubiquitous fibrils seen in this line are all chromospheric. They are partially evident also in Ca II 854.2 nm (Vecchio et al. 2007) and appear thicker in Ly- α (Korendyke et al. 2001; Vourlidas et al. 2001; <http://wwwsolar.nrl.navy.mil/rockets/vault>) but H α remains the principal diagnostic of this regime.

Figure 2 illustrates that diagnostic usage of H α requires sampling its line profile. The blue-wing scene at the right differs markedly from the line-centre scene at the left by selectively showing the more upright spicular fibrils jutting out from the network. Their darkening is due to a combination of source func-

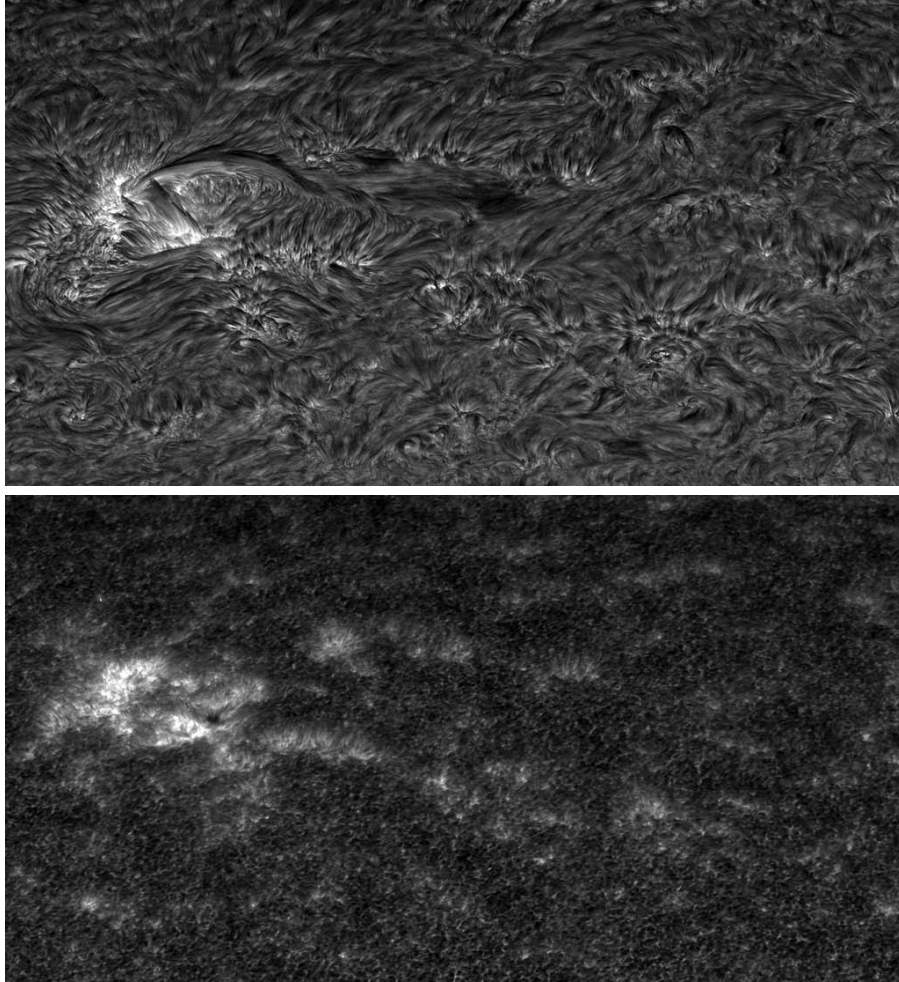


Figure 1. Simultaneous $H\alpha$ and $Ca\text{II}H$ images taken by P. Sütterlin with the DOT. The field of view is close to the limb (off the top) and measures about $265 \times 143 \text{ arcsec}^2$. From Rutten (2007).

tion, opacity, Doppler shift, and Doppler broadening variations. Only profile sampling can disentangle these.

2. $H\alpha$ Ubiquity = Shocks + Sluggish Recombination + Ion Coupling

Figure 3 is from Leenaarts et al. (2007) in which for the first time non-equilibrium ionization of hydrogen was computed within a 2D MHD simulation of the solar atmosphere including its influence on the equation of state. The resulting dynamical structure and behaviour of the chromosphere differ markedly from those in a parallel classical simulation assuming instantaneous LTE partitioning.

The physics of non-equilibrium hydrogen ionization was analyzed earlier by Carlsson & Stein (2002) using a 1D radiation-hydrodynamics simulation. The ionization/recombination balancing time scale is mainly set by the slow collision

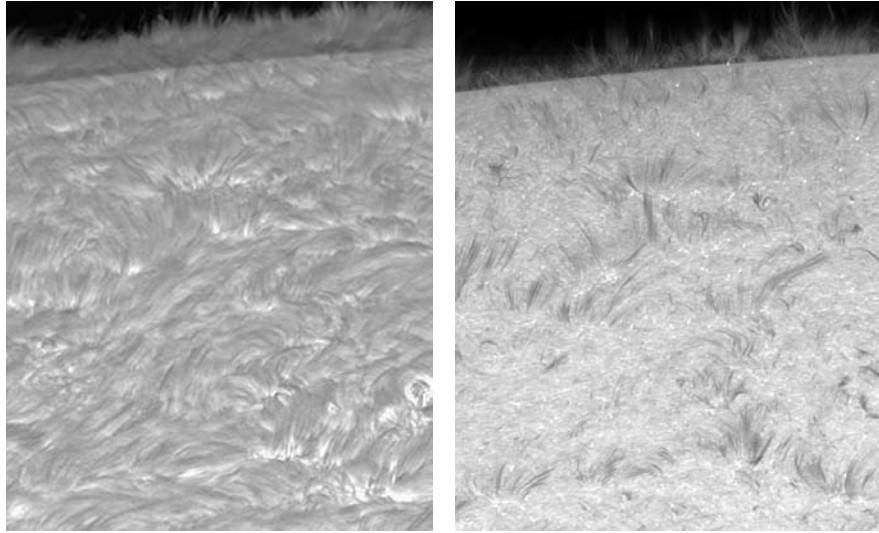


Figure 2. $H\alpha$ fine structure near and at the limb, taken by P. Sütterlin with the DOT on October 4, 2005. Left: line centre. Right: $\Delta\lambda = -800$ mÅ. Field of view about 70×85 arcsec². From Rutten (2007).

rate from $n=1$ to $n=2$ (which is followed by Balmer photoionization). This rate is slow for lack of 10 eV electrons unless the temperature gets high. Therefore, hydrogen gets ionized in hot shocks but does not recombine swiftly enough in the cool post-shock phases to reach balancing corresponding to the low temperature there before the next shock comes along.

Panels a and b of Figure 3 show that both the network and the inter-network chromosphere are pervaded by upward propagating successive shocks, slanted into dynamic fibrils in the network and pushing up a high-lying $\beta = 1$ canopy and transition region in the internetwork. Panels c and d show that the degree of hydrogen ionization is set by the high-temperature spikes, also during the low-temperature post-shock phases. The corresponding NLTE population departures reach b values as high as 10^{15} ! The ion population behaviour (panels e and f) is closely mimicked by the $n = 2$ population behaviour (panels g and h) because the upper hydrogen term structure is closely coupled to the ion population (Rutten & Carlsson 1994). The result is that $H\alpha$ has very much more opacity in the cool phases than LTE would predict. *$H\alpha$ is ubiquitously present because shocks are ubiquitously present.* Similarly, it is likely that the cool phases do not show up in Ca II H (Fig. 1) due to lack of recombination from Ca III, whereas Saha-Boltzmann predicts much larger Ca II H than $H\alpha$ opacity.

3. DOT co-pointing with *Hinode*

Hinode's $H\alpha$ imaging is in some cases affected by bubbles. Also, *Hinode's* on-board memory and telemetry limit the possibilities to perform the long-sequence fast-cadence full-profile sampling needed to fully exploit $H\alpha$. In good seeing the DOT reaches the same angular resolution as *Hinode* obtaining $H\alpha$ image sequences with multi-wavelength line profile sampling at cadences ≈ 15 s. Thus,

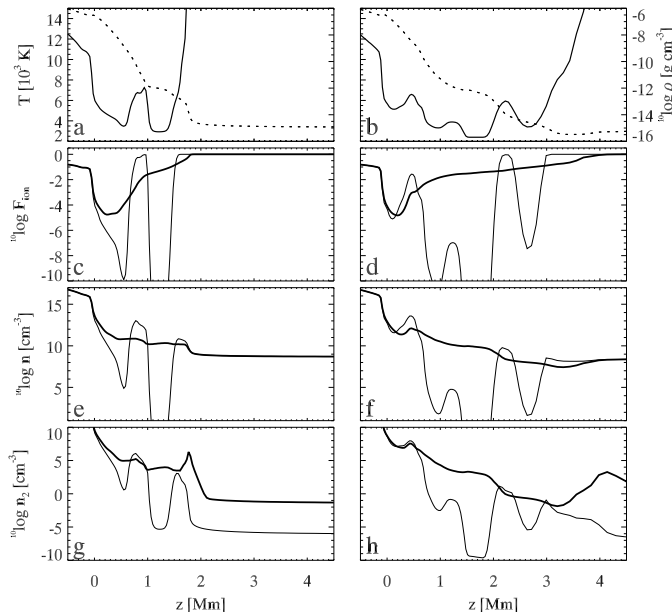


Figure 3. Vertical stratifications in a snapshot from a 2D MHD simulation of the solar atmosphere above a network element (left) and above internetwork (right). Panels a and b: temperature (solid) and density (dashed, scale at right); c and d: non-equilibrium (thick) and LTE hydrogen ionization degree (thin); e and f: non-equilibrium (thick) and LTE hydrogen ion density (thin); g and h: population of the HI $n=2$ level for the non-equilibrium (thick) and LTE (thin) case. From Leenaarts et al. (2007).

co-pointing the DOT and *Hinode* would partially remedy *Hinode*'s unfortunate lack of chromospheric diagnostic capability.

However, Utrecht University does not continue its principal DOT sponsorship beyond 2007. The above considerations give scientific motivation to continue DOT observing nevertheless. Our present funding prospects are that we will manage to keep the telescope functional, but without an on-site observer to take and process data. Proposals to solve this problem are welcome.

References

- Carlsson M., Stein R. F. 2002, ApJ, 572, 626
 Korendyke C. M., Vourlidas A., Cook J. W., Dere K. P., Howard R. A., Morrill J. S., Moses J. D., Moulton N. E., Socker D. G. 2001, Solar Phys. , 200, 63
 Leenaarts J., Carlsson M., Hansteen V., Rutten R. J. 2007, A&A, 473, 625
 Rutten R. J. 2007, in P. Heinzel, I. Dorotovič, R. J. Rutten (eds.), The Physics of Chromospheric Plasmas, ASP Conf. Series 368, 27
 Rutten R. J., Carlsson M. 1994, in D. M. Rabin, J. T. Jefferies, C. Lindsey (eds.), Infrared Solar Physics, IAU Symp. 154, 309
 Vecchio A., Cauzzi G., Reardon K. P., Janssen K., Rimmele T. 2007, A&A, 461, L1
 Vourlidas A., Klimchuk J. A., Korendyke C. M., Tarbell T. D., Handy B. N. 2001, ApJ, 563, 374